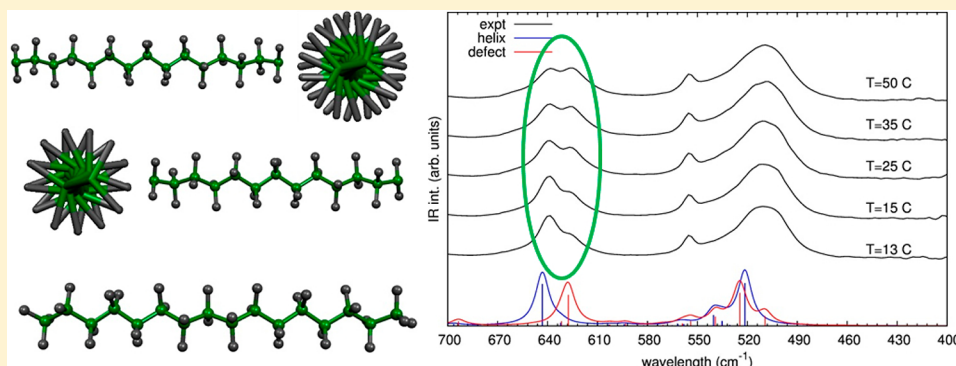


Ab Initio Calculation of the IR Spectrum of PTFE: Helical Symmetry and Defects

Claudio Quarti,* Alberto Milani, and Chiara Castiglioni

Politecnico di Milano – Dip. Chimica, Materiali e Ing. Chimica “G. Natta”, P.zza Leonardo da Vinci 32, I-20133 Milano, Italy

Supporting Information



ABSTRACT: A detailed analysis of the structure and vibrational properties of PTFE and the assignment of its IR spectrum are carried out by means of density functional theory simulations on infinite, one-dimensional chains. Calculations take into consideration regular polymer chains with different conformations (15_7 , 13_6 , 10_3 , 4_1 , and 2_1) in order to investigate the main features due to the peculiar helical structures in the IR spectra. In addition, also the helix-reversal defect and effects related to conformational disorder are considered, to analyze the contributions in the spectrum due to defects and to the amorphous phase. The present study solves the ambiguities in the interpretation of the $638\text{--}626\text{ cm}^{-1}$ doublet, assigning the lower frequency component to a normal mode of the helix-reversal defect. This interpretation is consistent with the general belief that the PTFE crystal contains a large concentration of defects already at low temperature and that the two crystalline transitions at room temperatures (19 and 30°C) are accompanied by an order-disorder transition. As an additional result, the 788 cm^{-1} band, previously adopted to measure the amount of amorphous material in real samples, is confirmed as a marker of this phase.

1. INTRODUCTION

In spite of the wide range of applications and the large amount of scientific literature dealing with the fundamental and technological properties of poly(tetrafluoroethylene) (PTFE), this polymer still presents some debated issues concerning its structural and spectroscopic characterization. Furthermore, a thorough understanding of its molecular properties is desirable, since PTFE is the simplest fluorinated polymer and it is often considered as a model in structural and spectroscopic studies of the many new advanced fluorinated materials.¹

The difficulty encountered in the definition of the PTFE structure is related to the occurrence of several phase transitions in a rather small range of temperatures ($0\text{--}50^\circ\text{C}$), in which conformational disorder is observed in the crystalline phase, coexistent with fully amorphous regions. The different crystalline phases are characterized by a different chain conformation and/or by a different three-dimensional arrangement of the polymer chains in the crystal cell. Two regular conformations of the chain have been identified, namely, a 13_6 helix found in form II, stable below 19°C , and a 15_7 helix at temperatures higher than 19°C .^{2a} Between 19 and 30°C , the 15_7 chains are packed in a hexagonal structure (form IV) which goes through a transition to a

pseudohexagonal structure above 30°C (form I).^{2b} Another crystalline form (form III) is reported for samples obtained by crystallization under high pressure and is characterized by the transplanar conformation of the polymer chains.^{3,4} The smearing of the XRD peaks going from form II to IV to I has been interpreted as due to an increase of the structural disorder in the higher temperature phases. According to the early paper of Rigby and Bunn, “there is an evident change of crystal structure; it is, however, not a change from one precise arrangement to another, but a change from a 3-dimensional (fully crystalline) order below 20°C to a lower degree of order above 20°C ”.^{5a} However, DSC measures on PTFE demonstrated that the observed phase transitions happen at well-defined temperatures.⁶

In addition to X-ray diffraction studies,^{2,5,7} also vibrational spectroscopy^{4,8–13} has been used for the structure characterization of PTFE, providing in some cases contrasting interpretations of the few, often broad and overlapped vibrational features. Krimm and Liang carried out a first assignment of the IR

Received: October 16, 2012

Revised: December 14, 2012

Published: December 17, 2012

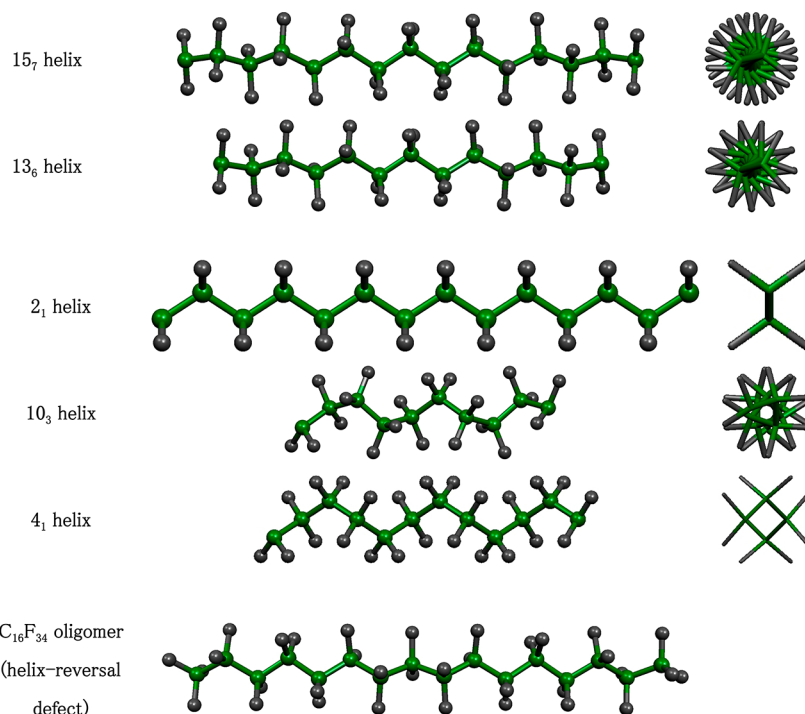


Figure 1. Sketches of the infinite and finite length model systems adopted in the computational study. The helix models have been investigated by means of the CRYSTAL09 code²⁰ taking into account explicitly the helical symmetry; the helix-reversal defect has been investigated by means of GAUSSIAN09 code²¹ by considering $C_{16}F_{34}$ and $C_{28}F_{58}$ oligomers. Only the $C_{16}F_{34}$ model is drawn. Carbon atoms are painted in green and fluorine atoms in gray.

spectrum of PTFE on the basis of the 13_6 helical structure of the chain.⁸ Successively, Moynihan revised the assignment of a few bands; moreover, he suggested that the intensity ratio between the 778 and 2367 cm^{-1} bands could be used for a measure of the degree of crystallinity of PTFE samples⁹ and this method finds practical application still nowadays.¹⁴

The relative IR intensity of the $638\text{--}626\text{ cm}^{-1}$ doublet is the only spectral feature that shows a significant evolution with the temperature. In correspondence of the crystal transitions, going from 19 to $30\text{ }^{\circ}\text{C}$, the 638 cm^{-1} component decreases in intensity, while the 626 cm^{-1} component increases. Moynihan associated this variation to the transition between the crystalline form, showing a 13_6 (form II) conformation of the chain and the phases characterized by the 15_7 helix (forms IV and I).⁹ Accordingly, the peak at 638 cm^{-1} was associated to the former phase and the peak at 626 cm^{-1} to the latter. Subsequently, this interpretation was debated by Brown,⁴ who noticed that the change of the intensity ratio in the $638\text{--}626\text{ cm}^{-1}$ doublet is not limited to the temperature ranges characteristic of the phase transformations: indeed, an absorption feature at 626 cm^{-1} is also present well below $19\text{ }^{\circ}\text{C}$, and its intensity steadily increases until $50\text{ }^{\circ}\text{C}$. On this basis, Brown assigned the 626 cm^{-1} band to the formation of a helix-reversal defect,⁴ which can be easily arranged in the crystal.

In the same period, De Sanctis et al. carried out a theoretical study on the conformation potential of PTFE, as a function of the torsional angle (θ) around the CC bond. On the basis of molecular mechanics (empirical potential energy functions), they obtained a symmetric potential curve with global minima at about $\pm 165^{\circ}$ and local minima around ± 90 and $\pm 60^{\circ}$. Only one flat minimum was found around 165° ; thus, the presence of two stable conformations (the 15_7 and 13_6 conformations) cannot be taken into account on the basis of the conformational potential of

PTFE. In addition, the trans-planar conformation ($\theta = 180^{\circ}$) was found to be a maximum of the potential surface.¹⁵

In the 1970s, Koenig and co-workers carried out an extensive investigation on PTFE by means of Raman spectroscopy and they developed a specific empirical force field for the prediction of the vibrational frequencies.¹⁰ These authors concluded that no (Raman) spectroscopic markers associated to the phase transition at room temperature exist and they claimed for evidence of crystal splitting.^{10e} It is still not clear whether the low temperature phase (form II) contains one chain per cell^{15b} or two chains with different chirality;¹⁶ thus, the presence of crystal splitting cannot be ruled out.

A deep revision of the IR spectrum of PTFE was carried out by Zerbi and co-workers,¹³ by means of calculations based on the force field developed by Koenig et al.^{10c} Zerbi calculated $k = 0$ phonons and phonon dispersion curves of different helical structures. In connection with the results of De Sanctis,¹⁵ he considered the 15_7 , 10_3 , 4_1 , and planar 2_1 helical conformations. Accordingly, he predicted a band at 619 cm^{-1} for the planar 2_1 conformation. The assignment of this theoretical band to the observed feature at 626 cm^{-1} brought the hypothesis of the occurrence in the crystal of long sequences of CF_2 units in transplanar conformation. In addition, bands calculated for the PTFE helices characterized by the 10_3 and 4_1 conformations found a correspondence with the experimental bands at 288 and 778 cm^{-1} .

However, the question of the correct assignment of the lower frequency component of the IR doublet at $638\text{--}626\text{ cm}^{-1}$ remained unsettled until now, due to the lack of theoretical methods suitable for a deeper investigation of the problem. Nowadays, the availability of theoretical methods and computational quantum chemical codes suitable for the prediction and the interpretation of the vibrational spectroscopic features of crystalline polymers is well assessed.^{17,18} On this basis, in this

work, we revise the assignment of the IR spectrum of PTFE, thus settling the controversial issue on the assignment of the 626 cm^{-1} band and giving a deeper comprehension of the spectroscopic behavior of PTFE. Our calculations confirm the interpretation of Brown on the formation of the helix-reversal defects in PTFE. Moreover, they support the belief that the vibrational properties of PTFE are related to a transition to a more disordered crystalline phase at room temperature.^{7c}

The manuscript is organized as follows. In section 2, the models and the computational methods employed are presented. In section 3, we show the results of the calculations concerning both the molecular structures and the IR spectra of PTFE. In particular, in section 3.1, we revisit the work of Zerbi on polymer chains with different helical structures. Both infinite and finite model systems have been considered, respectively, in sections 3.1.1 and 3.1.2. In section 3.2, we discuss the helix-reversal defects. In section 3.3, we carry out a conformational analysis on PTFE oligomers, to discuss the contribution (in the IR spectrum) of the amorphous phase. Discussions and conclusions are reported, respectively, in sections 4 and 5.

2. COMPUTATIONAL DETAILS

Calculations of the equilibrium structures and of the IR spectra of PTFE are carried out in the framework of the density functional theory (DFT). PTFE is described as a single, isolated polymeric chain in regular conformation, similarly to a previous study on polystyrene.¹⁸ The choice of neglecting the supra-molecular arrangement is dictated by the fact that the structures on the 3-D crystal phases are still debated¹⁶ and intermolecular effects are expected to have small or negligible effects on the IR spectrum. In fact, if on one side the intermolecular interactions would give place to crystal splitting of some $k = 0$ bands in systems with more chains per unit cell, on the other side, the splitting can be hardly detected in the IR spectra of semicrystalline polymers, characterized by broad absorption bands, as is indeed the case of PTFE. On the opposite, the effects due to the intramolecular structure usually show clear signatures in the IR spectrum. Indeed, several examples are reported of studies where the presence of different conformers is observed by IR spectroscopy and the evolution of their relative population with temperature is monitored by IR intensity analysis;^{1a} moreover, the detection of conformational defects in polymeric materials has been successfully carried out for a long time through IR analysis.¹⁹ For the above reasons, we believe that the models adopted here (namely, single PTFE chains *in vacuo*) are reliable for the detailed investigation on the IR spectrum of PTFE.

DFT calculations are carried out on both infinite and finite models, sketched in Figure 1: calculations on the infinite polymeric chains are performed with CRYSTAL09 code,²⁰ which allows the helical symmetry to be taken into account explicitly. Calculations on finite oligomers are carried out with GAUSSIAN09 code.²¹

The hybrid B3LYP functional²² and Ahlrichs-TZVP basis set²³ were adopted. Calculations on both infinite and finite chains were repeated also with the widely used and cheaper B3LYP/6-31G(d,p)²⁴ method, in order to investigate the effect of the basis set; these results are reported in the Supporting Information. Since intramolecular dispersion effects can be important in different helices, we carried out calculations also by introducing the D2 semiempirical corrections developed by Grimme.²⁵ The effects on relative energies and spectra prediction are however completely negligible, as proven by the results reported in the Supporting Information.

Thin films of PTFE were kindly provided by Solvay Solexis; temperature controlled infrared absorption spectra were recorded with a Nicolet Nexus FT-IR spectrometer (resolution 1 cm^{-1} and 128 scans) on PTFE film placed in a Mettler FP82 Hot Stage cell.

3.1. RESULTS

3.1.1. IR Spectra of Infinite Polymeric Chains with Different Helical Structure. Calculations on infinite polymer chains of PTFE with different helical structures, proposed by Zerbi in the 1970s, are revisited here by using *state-of-the-art* electronic structure calculations (B3LYP/TZVP). In ref 13, the following helical structures, 15_7 , 10_3 , 4_1 , and the trans-planar 2_1 , were taken into account. Here, in addition to the above conformations, we consider also the 13_6 helical conformation, in order to investigate the transition from the low temperature 13_6 phase to the higher temperature 15_7 one. The different regular helix conformations of the infinite chain were selected by a symmetry constraint, which in turn determines the order of the rototranslational axis. The structural parameters were optimized for the various conformations, and they are reported in Table 1

Table 1. Equilibrium Repeating Distance, Torsional Angles, and Relative Energies of the 15_7 , 13_6 , 10_3 , 4_1 , and 2_1 Helical Structures of an Infinite PTFE Chain^a

helix	repeating distance (Å)	dihedral angle (deg)	energy (kcal/mol per CF_2 unit)
15_7	19.71	165.6	0.07
13_6	17.06	163.4	0.00
10_3	11.93	91.7	1.85
4_1	4.68	72.4	2.97
2_1	2.65	180.0	0.41

^aCalculations (B3LYP/TZVP) have been carried out with the CRYSTAL09 package by imposing PBC along the chain direction, with constrained helical symmetry.

together with the respective energies. Computed optimized geometries adequately reproduce the experimental data available for crystals showing the 15_7 and 13_6 conformation of the chains, characterized by a cell parameter along the polymer axis, respectively, of 19.5 and 16.88 Å and torsional angle around the CC bond of 165.8 and 163.5°.³

Considering the relative stability of the 15_7 and 13_6 helices, they are predicted to be quasi-isoenergetic, the latter being more stable than the former of less than 0.1 kcal/mol. However, calculations at a different level of theory (B3LYP/6-31G(d,p)) show the opposite trend, with the 15_7 more stable than the 13_6 by 0.04 kcal/mol (see Table SI1, Supporting Information).²⁶ Because of the small energy difference obtained for the two conformations, it is hard to discuss the relative stability of the 13_6 (phase II) and 15_7 forms (phases IV and I) on the basis of our theoretical predictions. However, we notice that the energy difference found between the two conformations is certainly comparable to the dispersion interactions between the different chains packed in the crystal. This fact is somehow consistent with the interpretation of Strobl, who suggested that the low temperature 13_6 phase is dominated by intermolecular interactions, while the high temperature 15_7 phase is dominated by intramolecular interactions.^{7c}

Our calculations show that helices with the 10_3 or 4_1 conformation lie higher in energy; namely, the formation of a single helical turn requires more than 10 kcal/mol. Finally, the 2_1

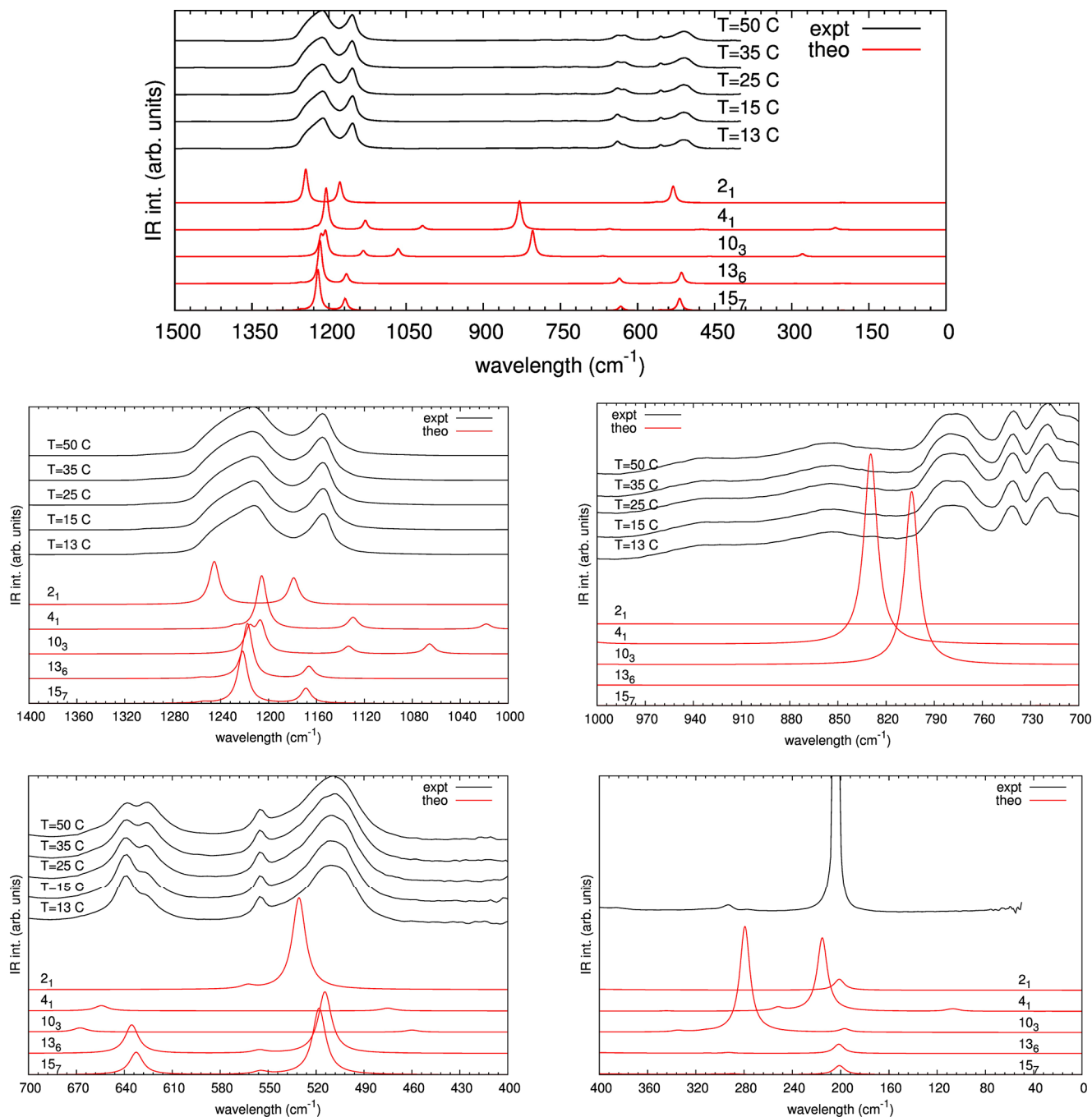


Figure 2. Comparison of the experimental spectra of PTFE recorded at various temperatures and the theoretical spectra calculated on the 15_7 , 13_6 , 10_3 , 4_1 , and 2_1 helical structures for the infinite chains. The B3LYP/TZVP functional/basis set is used. No scaling factor for the frequencies is used. Theoretical intensities are normalized to one CF_2 group and different intensity scales are adopted in the different spectral range, for a better visualization.

helical conformation is associated to a local maximum in the potential energy surface for symmetry reasons,^{15,27,28} and its energy determines the energetic barrier between the left and right 13_6 helical conformations, which results in being of the order of $k_B T$ (at room temperature), thus supporting the possibility of the formation of helical reversal defects, as proposed by Brown.⁴

In Figure 2, we compare the IR spectra calculated for the various helix models (15_7 , 13_6 , 10_3 , 4_1 , 2_1) with experimental spectra recorded at different temperatures (from 13 to 50 °C); for a correct comparison, the IR intensities of the theoretical spectra are normalized to one CF_2 group, while the intensity scale

adopted for the experimental spectra is arbitrary. The choice of the basis set does not affect the general pattern of the spectra, even if the use of the 6-31G(d,p) basis set red-shifts slightly the frequency of the bands in the CF stretching region (see Figure S11, Supporting Information). IR spectra computed for the 15_7 and 13_6 conformations are very similar and nicely reproduce the experimental features in the whole spectral region, with the exception of the region between 1000 and 700 cm^{-1} , that is traditionally associated to the amorphous phase (in this region, the experimental spectra have been magnified in order to clearly show the absorption features). Frequency differences between

the IR spectra calculated for the $1S_7$ and 13_6 conformations are in general very small, amounting to 5 cm^{-1} in the worst case.

Focusing on the region of the doublet at $638\text{--}626\text{ cm}^{-1}$, we notice that, going from the 13_6 to $1S_7$ conformation, the calculated band actually red-shifts from 636 to 632 cm^{-1} . Even if the predicted frequency shift (4 cm^{-1}) is small with respect to the splitting of the doublet experimentally observed (12 cm^{-1}), one could tentatively assign the two peaks of the experimental spectra to the different crystalline phases (forms II and IV), characterized by a change in chain conformation. However, the assignment of the two peaks to the 13_6 and $1S_7$ helices has already been rejected by many authors,^{4,13} since the variation of the relative IR intensity of the two components of the doublet extends well outside the range of temperatures characteristic of the phase transition. Accordingly, we state that, also on the basis of our theoretical predictions, no IR markers of transition from 13_6 to $1S_7$ helices of PTFE can be proposed.

In ref 13, the band at 626 cm^{-1} was assigned to a planar 2_1 helical structure: as shown in Figure 2 (region $700\text{--}400\text{ cm}^{-1}$), no IR active bands are present for the 2_1 conformation in this suitable spectral range. One vibrational mode associated to such a conformation is predicted by our calculations in this region (615 cm^{-1}), but it is not IR active, since it belongs to B_{1g} symmetry. Thus, the previous assignment should be revised according to the present DFT results.

On the other hand, in agreement with previous assignments,¹³ we find that some bands calculated for the 10_3 and 4_1 conformations nicely reproduce the 740 and 778 cm^{-1} experimental absorptions in a spectral region assigned to the amorphous phase. Also, the original assignment of the IR band at 288 cm^{-1} to the 10_3 conformation finds a parallel in our calculations. It is difficult, at this stage of our investigation, to state whether the occurrence of some absorption bands in the $1000\text{--}700\text{ cm}^{-1}$ range reveals the presence of long chain sequences in a peculiar regular helix conformation (namely, 10_3 or 4_1 helices) or can be better explained as originated by disordered conformations occurring in the amorphous phase, containing isolated gauche defects (i.e., with some torsional angle close to $\pm 60^\circ$). Since this point deserves a deeper investigation, an analysis of the absorption features in the $1000\text{--}700\text{ cm}^{-1}$ region will be done in the section 3.3, by means of a conformational analysis of PTFE oligomers.

3.1.2. IR Spectra of Finite Oligomers with Different Helical Structures. In parallel with the previous calculations on infinite systems, we carried out geometry optimization and calculation of the IR spectrum also on some oligomeric models of PTFE, characterized by the same helical structures adopted for the study of the 1-D crystal. This analysis was done in order (i) to make a comparison with the results previously obtained on infinite systems to check the consistency of the two computational approaches adopted and (ii) to provide information about the effect of the confinement due to the finite size of molecules. The issues described in (i) and (ii) are particularly important in the perspective of the subsequent studies on finite size models and aimed to identify spectroscopic markers of structural defects, such as the helix-reversal defect and conformational disorder typical of the amorphous phase.

As in the works of Barone and co-workers,²⁹ the oligomer $C_{16}F_{34}$ was taken as a model: five relevant helical conformations, namely, $1S_7$, 13_6 , 10_3 , 4_1 , and 2_1 helices, were constrained by fixing the torsional angles of the oligomer to the values found for the infinite models, reported in Table 1. Then, the molecular geometry has been optimized by keeping fixed all the torsional

angles of the polymer backbone. In addition, a full molecular optimization without constraints on torsional angles was carried out, using as a guess structure the most stable helical conformation, i.e., the 13_6 helix.

Calculations on the five $C_{16}F_{34}$ oligomers obtained according to the different helical structures considered show relative energies that follow the same trend found in the case of the infinite helices, as reported in Table 2. This is an indication that

Table 2. Equilibrium Dihedral Angles and Relative Energies per CF_2 Group of the Fully Optimized (OPT) and of the $1S_7$, 13_6 , 10_3 , 4_1 , and 2_1 Helical Structures of the Finite $C_{16}F_{32}$ Oligomer^a

helix	dihedral angle (deg)	energy (kcal/mol per CF_2 unit)
OPT	161.8	
$1S_7$	165.6	0.20
13_6	163.4	0.07
10_3	91.7	1.47
4_1	72.4	2.16
2_1	180.0	0.48

^a Calculations were carried out with the GAUSSIAN09 package (B3LYP/TZVP).

results obtained for the $C_{16}F_{34}$ model can be considered consistent with those obtained on the infinite chain. The fully optimized structure shows a geometry very similar to the 13_6 conformation, with torsional angles of about 162° .

IR spectra of the $C_{16}F_{34}$ oligomer constrained in the five different helical structures were calculated and are reported in Figure 3, where a comparison with spectra calculated for the infinite chains is also shown. A procedure used in some of our previous works,^{1b} that consists of computing vibrational spectra for molecules carrying fictitious heavy masses at the terminal CF_3 groups, allows one to avoid spurious features due to terminal CF_3 groups and to obtain a spectrum which can be compared with that of the infinite chain straightforwardly. The results of the calculations on the finite $C_{16}F_{34}$ system parallel those of the infinite systems, especially in the region of the doublet $638\text{--}626\text{ cm}^{-1}$. On the opposite, the weak bands calculated at 740 and 720 cm^{-1} for the 13_6 and $1S_7$ conformations of the oligomer do not parallel any feature of the corresponding infinite chain. On this basis, the experimental bands at 740 and 720 cm^{-1} could be associated to finite chain effects.

While the spectra calculated with the two approaches (on infinite and finite systems) do not match perfectly in frequency, calculations on longer oligomers (30 CF_2 units), carried out with the B3LYP/6-31G(d,p) (Figure S12, Supporting Information) basis set, reproduce very well the results obtained for the infinite systems at the same level of theory. This suggests that the frequency mismatch shown by the spectra reported in Figure 3 has to be ascribed exclusively to effects due to the finite length of the chain.

In light of the calculations on the oligomers, we can confirm the relevant conclusion of section 3.1.1. No intense IR bands associated to sequences in all trans conformation are predicted in correspondence of the doublet at $638\text{--}626\text{ cm}^{-1}$; moreover, in this region, also in the case of the oligomer the 2_1 helical structure shows just one, IR inactive (B_{1g}) band.

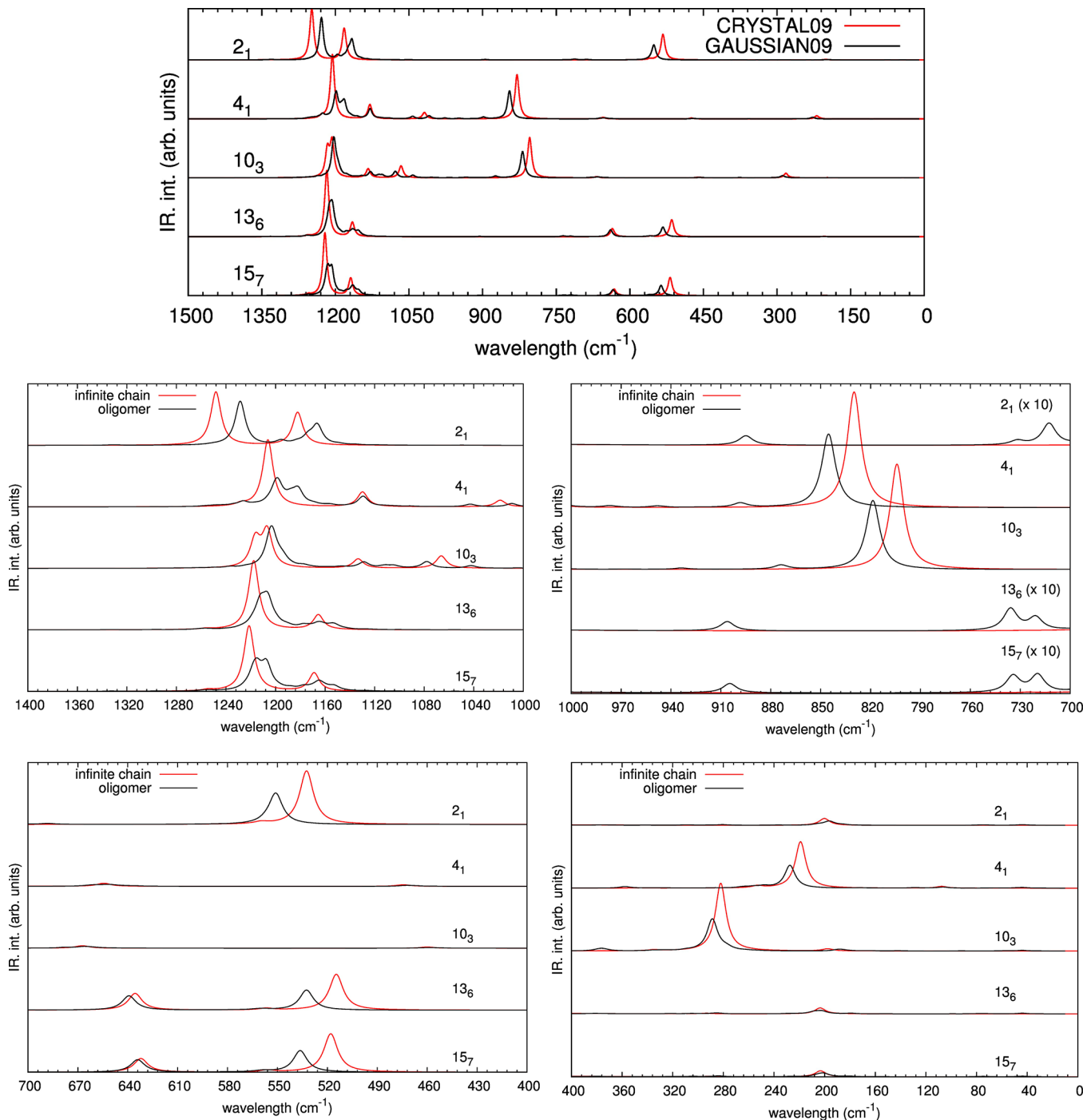


Figure 3. Comparison between the spectra calculated on infinite PTFE chains (CRYSTAL09) and on the $C_{16}F_{34}$ oligomer (GAUSSIAN09), for the 15_7 , 13_6 , 10_3 , 4_1 , and planar 2_1 helical structures (B3LYP/TZVP). No scaling factors for frequencies are used. Theoretical intensities are normalized to one CF_2 group (except for the region 1000 – 700 cm^{-1} , where the intensities for the 15_7 , 13_6 , and 2_1 helical structures have been amplified by a factor of 10) and different intensity scales are adopted in the different spectral range, for a better visualization.

3.2. HELICAL REVERSE DEFECT

In this section, we will take into consideration the interpretation of Brown, according to which the 626 cm^{-1} band is associated to the formation of a helix-reversal defect.⁴

A model for the helix-reversal defect has been proposed recently by Barone and co-workers, based on DFT calculations.²⁹ They considered the $C_{16}F_{34}$ oligomer as representative of the PTFE chain, and they obtained a stable conformation of the type ... $t^+t^+t^+(t^*)^*t^-t^-$..., where $t^\pm = \pm 162.4^\circ$ and $(t^\pm)^* = \pm 172.2^\circ$.

(optimization performed with GAUSSIAN09 at the PBE0/6-31G(d) level). In the present work, in addition to the $C_{16}F_{34}$ oligomer, we consider also the longer oligomer $C_{28}F_{58}$, in order to investigate the effect of increasing chain lengths on the IR spectrum of the PTFE helix with the reversal defect.³⁰

For both oligomers, we started with a similar guess geometry: ... $t^+t^+t^+t^-t^-$... (where $t^\pm = \pm 160^\circ$). Then, we performed a full optimization at the B3LYP/TZVP level. The helical reversal is preserved during the optimization, and the system finally converged to a conformation very similar to that obtained by

Table 3. Torsional Angles Obtained for (i) the Fully Optimized Helical Structure (Helix) and (ii) the Helix-Reversal Defect (Defect) Model in $C_{16}F_{34}$ and $C_{28}F_{58}$ Oligomers^a

$C_{16}F_{34}$								
	θ_1	θ_2	θ_3	θ_4	θ_5	θ_6	θ_7	θ_8
helix	169.2	162.6	161.8	161.8	161.8	161.8	161.8	161.8
defect	169.2	163.0	161.7	161.7	161.5	160.6	169.2	-173.6
	θ_9	θ_{10}	θ_{11}	θ_{12}	θ_{13}	θ_{14}	θ_{15}	
helix	161.8	161.8	161.8	161.8	161.8	162.6	169.2	
defect	-161.6	-161.3	-161.7	-161.8	-161.8	-162.6	-169.2	
$C_{28}F_{58}$								
	θ_1	θ_2	θ_3	θ_4	θ_5	θ_6	θ_7	θ_8
helix	169.2	162.6	161.8	161.8	161.8	161.8	161.8	161.8
defect	169.2	162.6	161.8	161.8	161.8	161.8	161.8	161.9
	θ_9	θ_{10}	θ_{11}	θ_{12}	θ_{13}	θ_{14}	θ_{15}	θ_{16}
helix	161.8	161.8	161.7	161.9	161.7	161.9	161.7	161.9
defect	161.7	161.8	161.6	161.7	160.9	171.2	-171.5	-161.0
	θ_{17}	θ_{18}	θ_{19}	θ_{20}	θ_{21}	θ_{22}	θ_{23}	θ_{24}
helix	161.7	161.8	161.7	161.8	161.8	161.8	161.8	161.8
defect	-161.4	-161.7	-161.8	-161.8	-161.9	-161.8	-161.8	-161.8
			θ_{25}		θ_{26}			θ_{27}
helix			161.8		162.6			169.2
defect			-161.8		-162.6			-169.2

^aDihedral angles are labeled by increasing integer numbers starting from one end group and moving toward the other (B3LYP/TZVP).

Barone and co-workers. Thus, we can confirm that the helix-reversal defect is actually a local minimum of the potential energy surface of both the $C_{16}F_{34}$ and $C_{28}F_{58}$ oligomers.

In Table 3, we compare the values of the torsional angles calculated for the “regular” oligomers and for the same oligomers carrying the helix-reversal defect, as obtained through geometry optimization of $C_{16}F_{34}$ and $C_{28}F_{58}$. Notice that, with the exception of the end torsional angles, the fully optimized “regular” structures show a geometry closer to that of the 13_6 conformation ($\theta = 163.4^\circ$) than that of the 15_7 one ($\theta = 165.6^\circ$). In the molecules showing helix-reversal, the defect is quite localized and only two dihedral angles in the middle of the helix are markedly different from the optimum value characteristic of the regular structure. In particular, these angles relax to values (about $\pm 170^\circ$) close to 180° , which is the torsional angle characteristic of the trans-planar conformation (helix 2_1). The computed relative energy of the molecule with the helix-reversal defect is found to be 1.50 kcal/mol larger than that of the fully optimized regular chain, for both $C_{16}F_{34}$ and $C_{28}F_{58}$ oligomers. This result is in agreement with the value of 1.25 kcal/mol obtained empirically by Brown from the analysis of the IR spectra⁴ and with the value of 1.14 kcal/mol found by Barone et al. by means of DFT calculations at the PBE0/6-31G(d) level.²⁹

In Figures 4 and 5, we compare the IR spectrum calculated for the regular helical structure and for the helix-reversal defect, respectively, in the case of $C_{16}F_{34}$ and $C_{28}F_{58}$. In the same figures, the experimental spectrum of PTFE is shown, for the sake of comparison. The IR spectra computed for the helix-reversal defect and for the regular helical structure are quite similar in the CF stretching region: indeed, both $C_{16}F_{34}$ and $C_{28}F_{58}$ show a slight change in the intensity pattern, but no spectroscopic markers clearly associated to the helix-reversal defect can be found in this region. The two bands at 740 and 720 cm⁻¹ (absent for the infinite model) find correspondence both in the spectrum computed for the helix-reversal defect and in that of the regular helical structure. As noted in the previous section, such bands can be attributed to finite chain effects, thanks to the activation of

phonons at $k \neq 0$ due to the breaking of the translational symmetry. Notice moreover that also the presence of a helix-reversal defect breaks the translational symmetry of a polymeric chain; i.e., it might induce the occurrence of transitions typical of chains of finite size, also for a long chain.

Similar arguments hold for the band at 288 cm⁻¹, which is not present in the spectrum of the infinite 13_6 chain, but it appears both in the spectrum of the finite regular chains and in that of molecules characterized by the helix-reversal defect. However, we must recall that in section 3.1.1 we showed that the 740, 720, and 288 cm⁻¹ experimental bands find a correspondence also with some bands for the 10_3 and 4_1 helical structures. Thus, two assignments can be proposed for these features: (i) finite size effects, due to the presence of short chains in the sample or simply induced by conformational defects (as for instance the helix-reversal one), and (ii) formation of helical segments with 10_3 or 4_1 conformations. Because of the large energy associated to the formation of helical segments characterized by the 10_3 and 4_1 conformations, we think that the mechanism related to the activation of phonons at $k \neq 0$ in short regular CF_2 sequences with 13_6 helix structure is more likely.

In the region between 700 and 400 cm⁻¹, we see that the IR band calculated at 520 cm⁻¹ actually decreases its intensity when the helical defect is formed. Also, this effect, due to the occurrence of additional transitions in the same spectral region, over which the IR intensity is redistributed resulting in a broader absorption band, can be considered a marker of the helix-reversal defect. It is pleasant to notice that a continuous decrease of the peak height of the corresponding experimental feature (at 520 cm⁻¹) has been observed while increasing the sample temperature in the range between 13 and 50 °C.

In the region of the doublet 638–626 cm⁻¹, a band characteristic of the helix-reversal defect of the $C_{16}F_{34}$ oligomer appears (see Figure 4), in very good correspondence with the lower component of the doublet. Similar results are found for the $C_{28}F_{58}$ oligomer (see Figure 5), where, in the case of the defected

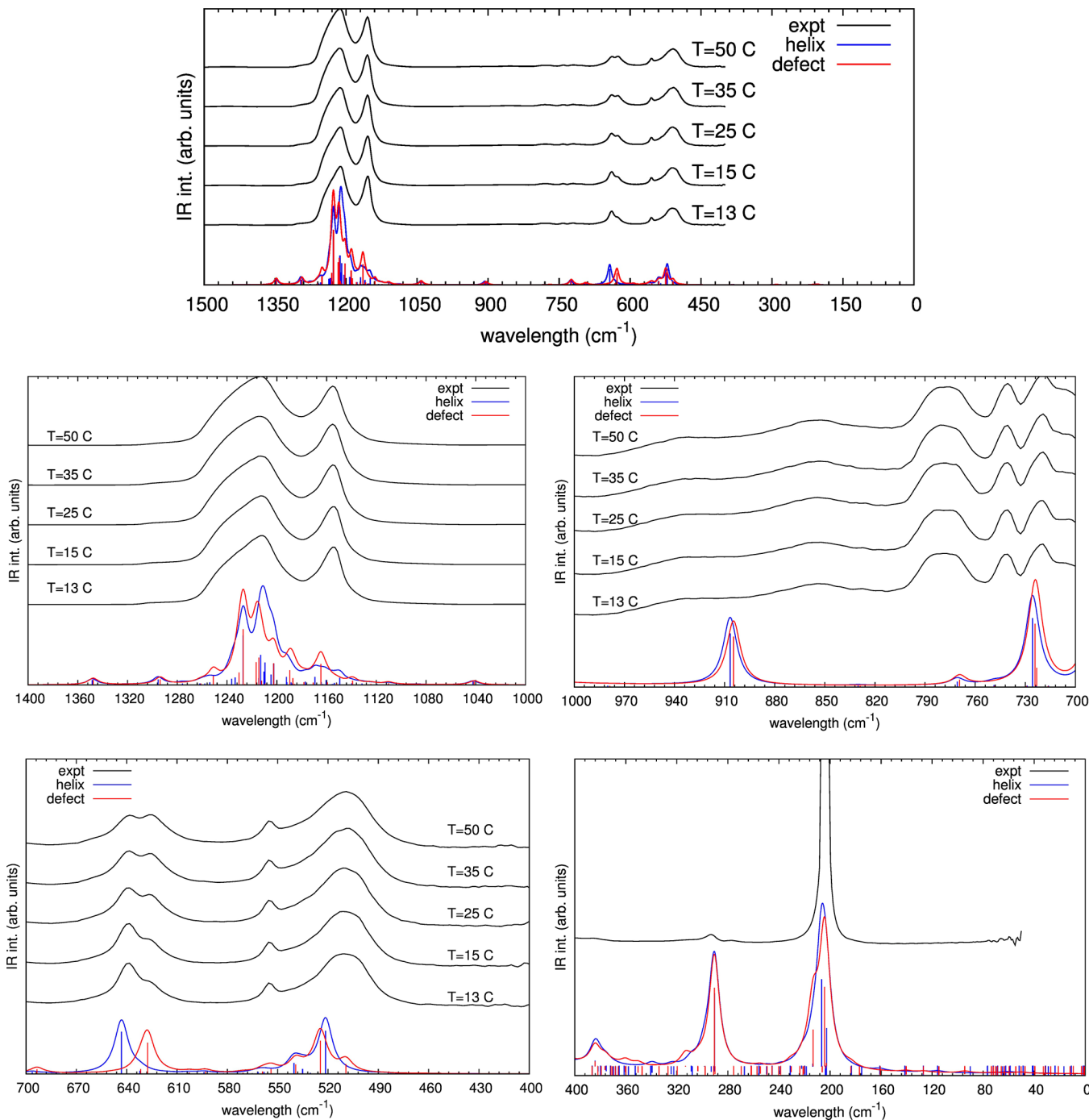


Figure 4. Comparison of the IR spectrum of $C_{16}F_{34}$ oligomer in two different optimized conformations: (i) regular helical structure; (ii) helix-reversal defect. Experimental spectra of PTFE at different temperatures are also shown. Calculations carried out with the GAUSSIAN09 package (B3LYP/TZVP). No scaling factor for the frequencies is used. Different intensity scales are adopted in the different spectral range, for a better visualization. Theoretical spectra have been obtained by assuming a Lorentzian band shape with a full width at half-maximum of 10 cm^{-1} .

molecule, two bands are predicted in correspondence of the observed doublet at $638\text{--}626\text{ cm}^{-1}$.

These results on oligomers strongly support the interpretation of Brown, namely, that the variation of the relative IR intensity of the doublet $638\text{--}626\text{ cm}^{-1}$ is due to the formation of a helix-reversal defect, whose population in the crystal increases as the temperature increases. Considering the short $C_{16}F_{34}$ chain, the lower component at 626 cm^{-1} is indeed definitely assigned to the helix-reversal defect and the higher component at 638 cm^{-1} is attributed to the regular helix. Notice instead that, in the case of

the longer $C_{28}F_{58}$ oligomer, the 638 cm^{-1} component gains intensity both from the chain in regular conformation and from the defected chain.

A further investigation, based on eigenvectors analysis, was carried out in order to better understand the behavior of the doublet. First, we report in Figure 6 the eigenvector of the band associated to the lower component of the $638\text{--}626\text{ cm}^{-1}$ doublet. As shown in Figure 6, this mode can be described mainly as CF_2 wagging vibration and it is quite localized on the

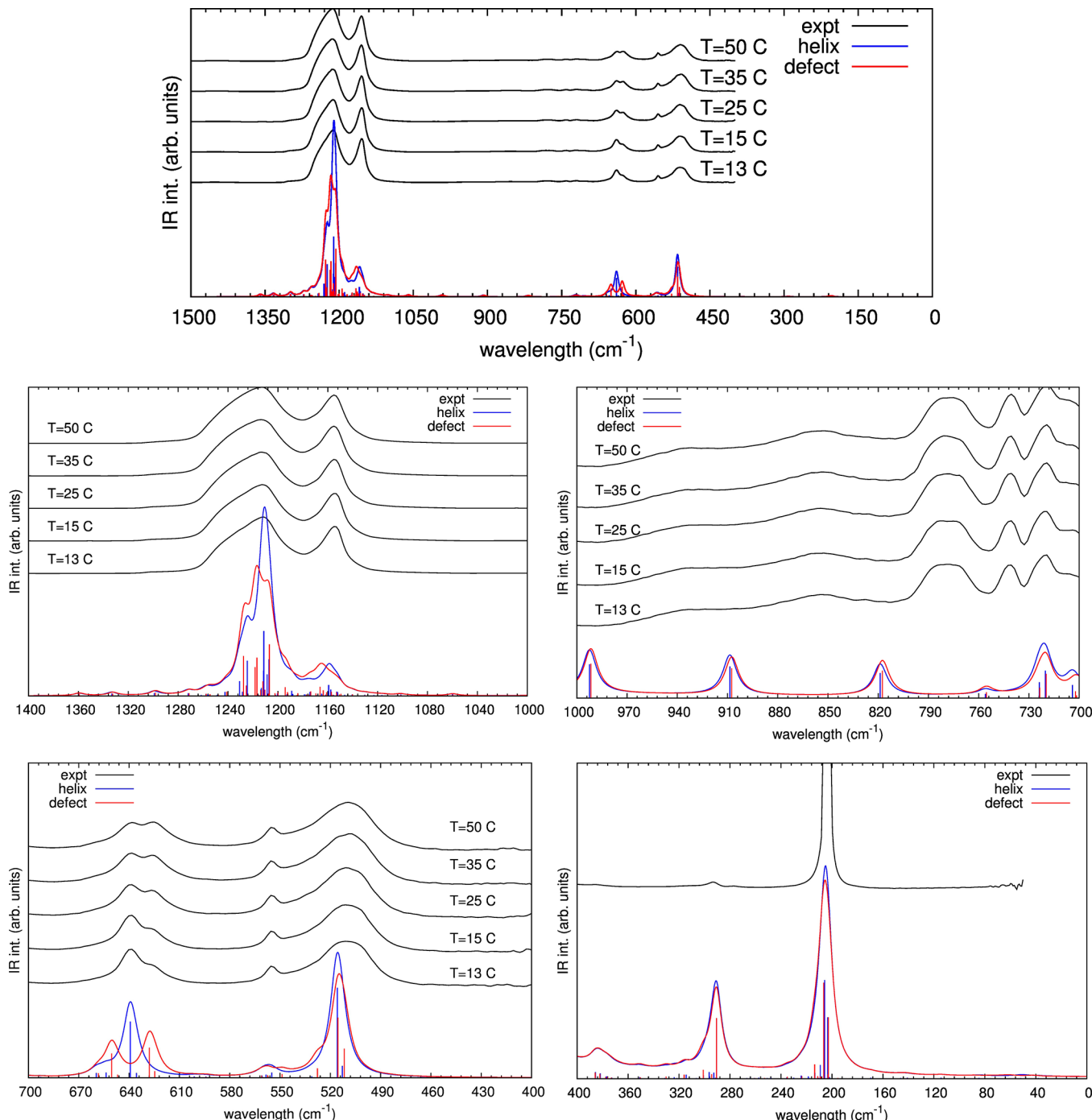


Figure 5. Comparison of the IR spectrum of $C_{28}F_{58}$ oligomer in two different optimized conformations: (i) regular helical structure; (ii) helix-reversal defect. Experimental spectra of PTFE at different temperatures are also shown. Calculations carried out with the GAUSSIAN09 package (B3LYP/TZVP). No scaling factor for the frequencies is used. Different intensity scales are adopted in the different spectral range, for a better visualization. Theoretical spectra have been obtained by assuming a Lorentzian band shape with a full width at half-maximum of 10 cm^{-1} .

seventh or eighth chemical units around the helix-reversal defect for both $C_{16}F_{34}$ and $C_{28}F_{58}$.

In Figure 7, we report the eigenvector associated to the high component of the doublet, for $C_{28}F_{58}$. A similar normal mode is found for the transition at 724 cm^{-1} predicted for $C_{16}F_{34}$, as shown in the same figure. The two normal modes sketched in Figure 7 can be described mainly as scissoring vibration of the CF_2 units, and they involve the whole chain and especially chemical units near the ends; their remarkable frequency shift can be ascribed to the different number of units involved, forming

a sequence with a regular helical conformation. On these grounds, we can argue that the 638 cm^{-1} band provides information about the coherence length of regular helical segments in real polymeric chains of PTFE. In Figure SI3 (Supporting Information), the IR spectrum calculated for oligomers of increasing length and containing helix-reversal defect is reported and the bands associated to vibrational modes with eigenvector similar to those reported in Figure 7 are highlighted.

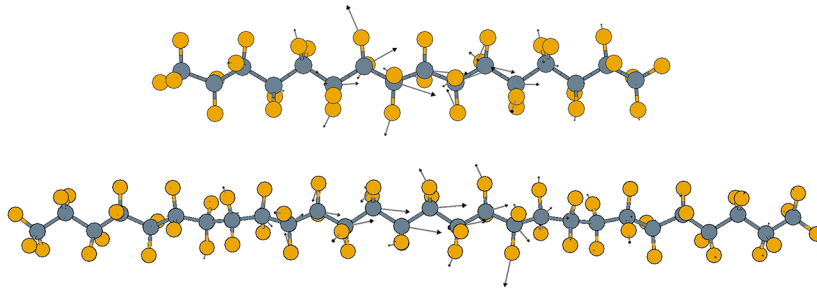


Figure 6. Eigenvectors associated with the band at 626 cm^{-1} as obtained from DFT calculations (B3LYP/TZVP) on $\text{C}_{16}\text{F}_{34}$ oligomer (upper panel) and on $\text{C}_{28}\text{F}_{58}$ (lower panel).

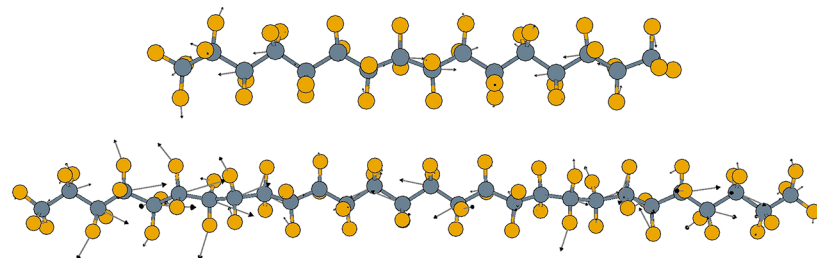


Figure 7. Eigenvectors associated with the band at 638 cm^{-1} as obtained from DFT calculations (B3LYP/TZVP) on $\text{C}_{16}\text{F}_{34}$ oligomer (upper panel) and on $\text{C}_{28}\text{F}_{58}$ (lower panel).

The selectivity of the helix-reversal defect (and that of its infrared marker band at 626 cm^{-1}) for a given kind of helix is another intriguing issue. In order to obtain some insight on this point, we studied the spectroscopic behavior of a helix-reversal defect on a chain characterized by both the 13_6 and 15_7 structures. Since a full optimization of a short chain always determines its relaxation into a structure with torsional angles of about 162° , it is necessary that all the torsional angles are kept fixed to the characteristic values reported in Table 1 for the 13_6 and 15_7 helices. For the two regular conformations, we calculated IR spectra for (i) the regular helical configuration and (ii) the chain carrying a helix-reversal defect in the middle, described as two segments characterized by the torsional angles of the 13_6 and 15_7 helices with opposite chirality and joined together. In other words, no relaxation for the torsional angles close to the helix-reversal defect was allowed. Calculations are carried out on the $\text{C}_{16}\text{F}_{34}$ oligomer. In Figure 8, the IR spectra of both (i) the regular helical configuration and (ii) the chain carrying a helix-reversal defect are compared in the region $700\text{--}400\text{ cm}^{-1}$. For each chain model, we found that the formation of the helix-reversal defect down-shifts the band at 640 cm^{-1} . The value of the frequency for the mode characteristic of the regular chain and of the defect band depends on the specific chain model adopted, but the computed frequencies always fall in the region of interest. Thus, we can conclude that the band at 626 cm^{-1} is not peculiar neither of the 13_6 nor of the 15_7 conformation.

3.3. CONFORMATIONAL STUDY

In order to evaluate the contributions of the amorphous phase to the IR spectrum of PTFE, we carried out a conformational study on a short oligomer. To this aim, we considered the C_8F_{18} oligomer as the best compromise between computational effort and accuracy needed to carry out a systematic investigation of the conformational space. The procedure for this analysis was the following. We constructed all the conformers which can be obtained by selecting, for each torsional angle, one of the following values: $0, 60, 120, 180, 240, 300^\circ$. In this way, we

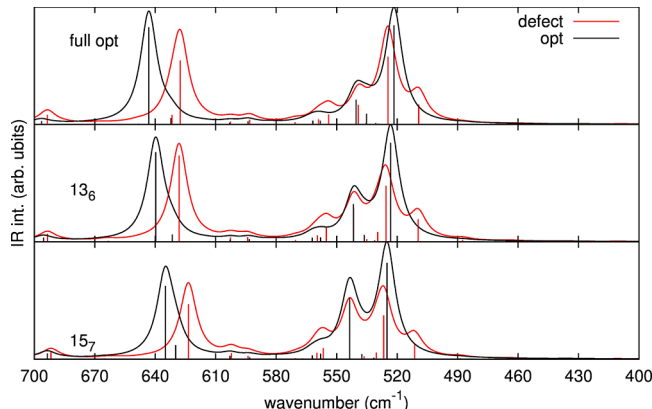


Figure 8. Comparison between the computed (B3LYP/TZVP) IR spectra for the $\text{C}_{16}\text{F}_{34}$ oligomer in its regular conformation (black line) and with a helix-reversal defect (red line). The molecular geometries are obtained according to three different ways: (i, top panel) fully optimized structure; (ii, middle panel) constrained 13_6 conformation; (iii, bottom panel) constrained 15_7 conformation.

collected 5^6 conformers. The conformation of each of them was optimized at a low theoretical level, namely, RHF/3-21G(d). Among the different conformers obtained, we selected only those characterized by a relative energy which does not exceed more than 5 kcal/mol the energy of the most stable structure, namely, that showing a structure similar to the 13_6 helix. Starting from the geometries so selected, a more accurate optimization and the calculation of the IR spectrum were carried out at the B3LYP/TZVP level.

The conformational analysis highlighted the presence of 49 conformers within the energy range of interest, whose energies and conformations are reported in Table SI2 (Supporting Information). The theoretical IR spectrum characteristic of the amorphous phase reported in Figure 9 was obtained by summing the contribution from each conformer, weighted for its respective Boltzmann population at a given temperature, similarly to

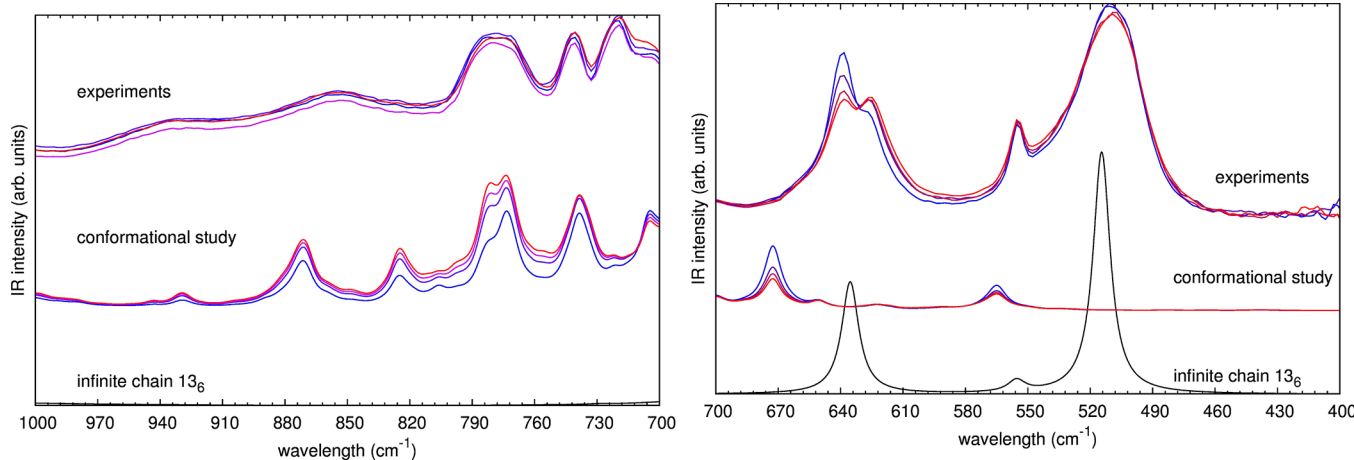


Figure 9. Comparison of the experimental IR spectra at various temperatures with those obtained by means of the conformational analysis of C_8F_{18} : the theoretical IR spectra are obtained by weighting the IR spectrum of each conformer with its corresponding Boltzmann statistical weight at different temperatures. The spectrum obtained for the infinite chain model 13_6 is also reported for the sake of comparison (B3LYP/TZVP).

previous studies.^{1a,31} We focus on the IR spectra of these conformers in the region between 1000 and 400 cm^{-1} in order (i) to discuss the possible contribution of the amorphous phase to the 638–626 cm^{-1} doublet and (ii) to analyze the region 900–700 cm^{-1} , traditionally associated to the amorphous phase. All the computed spectra are reported in Table SI3 (Supporting Information).

Dealing with the first point (see Figure 9, region 700–400 cm^{-1}), we observe that only a few conformers show IR bands in the region of the 638–626 cm^{-1} doublet, namely, conformer nos. 108, 138, 58, 46, 21, 61, and 55. All of these conformers are characterized by two gauche-like torsional angles at about 60 or 90°, excluding no. 55 that shows three torsional angles around 90°. However, all of these conformers lie at higher energy than that of the helix-reversal defect (at least 2 kcal/mol above the most stable 13_6 helix-like geometry), to be compared with 1.5 kcal/mol, corresponding to the energy needed to make the helix-reversal defect. Moreover, the computed intensity of the transitions which can be put in correspondence with the 626 cm^{-1} band are generally very weak. Only conformer no. 58 shows a band with IR intensity comparable to that shown by the helix-reversal model (43 vs 238 kcal/mol). In addition, a contribution of the amorphous phase to the steep increase observed for the 626 cm^{-1} band above 19 °C should be excluded because it would require a fast increase in the concentration of gauche-like defects in correspondence of the crystalline phase transitions (between 19 and 30 °C).^{7c} Such defects can be hardly hosted in a crystalline phase, characterized by parallel, well packed chains. Molecular dynamic simulations, made by Sprink and co-workers, showed that formation of gauche defects within ordered regions of PTFE occurs only at very high temperatures (hundreds of °C), that is, in a temperature range in proximity of melting.³² For all of these reasons, we believe that the contribution of the amorphous phase to the IR intensity of the 638–626 cm^{-1} doublet is negligible (see Figure 9, region 700–400 cm^{-1}).

Dealing with the second point (see Figure 9, region 1000–700 cm^{-1}), from the inspection of the IR spectra collected in Table SI3 (Supporting Information), we find many conformers that show intense bands in this spectral region. In particular, some predicted bands fall in correspondence with the experimental 740 and 720 cm^{-1} features, which were previously associated to phonons at $k \neq 0$. We believe that these bands get their intensity both from finite chain effects and from a truly amorphous phase.

In addition, many conformers show bands in correspondence with the 778 cm^{-1} broad band (conformer nos. 10, 26, 121, 113, 119, 79, 106, 38, 41, 115, 74, 7, 9, 68, 44, 61, 89, 99, 111, 32, and 34), that was associated by Moynihan⁹ to the amorphous phase; this interpretation is now confirmed by our present investigation.

4. DISCUSSION

The analysis presented in this paper allows to settle the assignment of the 638–626 cm^{-1} doublet in the IR spectrum of PTFE. The assignment of the 626 cm^{-1} band to the formation of trans-planar sequences¹³ can be definitely rejected because no IR active bands have been calculated for the 2_1 helical conformation in the spectral region of interest. The assignment proposed by Brown, who argued that the 626 cm^{-1} band is associated to the helix-reversal defect,⁴ is instead confirmed by our theoretical investigation. In fact, our calculations show that a stable structure associated to the helix-reversal defect exists, with energy of 1.5 kcal/mol above the energy of the most stable conformation (the 13_6 helix), in good agreement with the estimate from IR intensity measurements.⁴ In addition, the IR spectrum of this structure presents an IR active marker in correspondence to the lower component of the 638–626 cm^{-1} doublet.

This result confirms previous interpretations of the infrared features of PTFE, which have been attributed to the presence of structural disorder in crystalline PTFE, even at temperatures well below the melting point. In particular, based on the assignment of the 626 cm^{-1} feature to the helix-reversal defect, Kimmig and Strobl suggested that the transition from the 13_6 to the 15_7 helical conformation in PTFE is a transition from a state where intermolecular interactions are dominant to a state where intramolecular interactions prevail.^{7c} At low temperatures (lower than 19 °C), effective intermolecular interactions oppose the formation of helix-reversal and the concentration of these defects remains small. At the form II–form IV transition, the intermolecular interactions become less effective and thus the helix-reversal defects can easily develop, increasing in concentration until the thermodynamic equilibrium for the (quasi) isolated chain is reached. Accordingly, the transition at room temperature is better described as an order–disorder transition than as a true transition between different crystalline phases. This interpretation is consistent with the fact that crystal packing goes

from a triclinic structure in the 13_6 helix, that maximizes the intermolecular interactions of helical systems, to a hexagonal one for 15_7 helices.³ This structure indeed maximizes the packing of perfectly cylindrical objects, that is, for helices free to rotate.

Note that this interpretation is based on the assumption that the 13_6 conformation is stabilized by intermolecular interactions, while the 15_7 conformation is the true stable one, from a conformational point of view. Our calculations predict very small energy differences for these conformations (see Table 1), comparable with intermolecular interactions, but unfortunately, they cannot give a definitive validation to such an interpretation.

5. CONCLUSIONS

This work reanalyzes critically the interpretation of the IR spectrum of PTFE. Calculations with state-of-the-art methods for the prediction of the electronic and molecular structure are carried out at the aim of interpreting the experimental spectral features. Our calculations definitively settle the assignment of the $638-626\text{ cm}^{-1}$ doublet of PTFE as due to the formation of a helix-reversal defect, as proposed by Brown.⁴

The assignment of the bands at 740 , 720 , and 288 cm^{-1} to segments of helices with 10_3 and 4_1 conformation⁴ could be acceptable, but it seems not to be the main contribution because of the high energetic cost of these conformations (greater than 10 kcal/mol for helix turn). In fact, the experimental bands at 740 , 720 , and 288 cm^{-1} fall in correspondence with some transitions calculated for finite size chains (oligomers), with both helical structure and helix-reversal defects. On these grounds, the presence of such bands, showing constant IR intensity between 13 and $50\text{ }^{\circ}\text{C}$, can be taken as the evidence of the relatively low coherence length of the helix, already at low temperature.

As last useful result from a practical point of view, the assignment of the 778 cm^{-1} to the amorphous phase by Moynihan⁹ is confirmed by our analysis and then the use of the IR intensity of this band for a quantitative determination of the amount of amorphous material in real sample is supported by our theoretical results.

■ ASSOCIATED CONTENT

Supporting Information

Table with DFT computed equilibrium torsional angles and minimum energies of the 15_7 , 13_6 , 10_3 , 4_1 , and 2_1 helical structures of infinite chains. B3LYP/6-31G(d,p) and B3LYP/TZVP IR spectra of the 15_7 , 13_6 , 10_3 , 4_1 , and planar 2_1 conformations calculated on infinite polymeric chains. Comparison between the spectra calculated on infinite polymeric chains and on finite oligomers of about 30 CF_2 units for the different helices. IR spectra calculated for a different helical reversal defect. Table with the energy and conformation of the 49 conformers obtained from the conformational analysis. IR spectra calculated on the 49 conformers selected from the conformational analysis in the region between 1000 and 400 cm^{-1} . Tables with the optimized geometries of the different helices and tables with their DFT computed frequencies and IR intensities. This material is available free of charge via the Internet at <http://pubs.acs.org>.

■ AUTHOR INFORMATION

Corresponding Author

*E-mail: claudio.quarti@mail.polimi.it.

Notes

The authors declare no competing financial interest.

■ ACKNOWLEDGMENTS

The authors are grateful to Dr. Andrea Lucotti (Politecnico di Milano) and Dr. Stefano Radice (R&D Analytical & Structural Characterization - Solvay Specialty Polymers Italy SpA) for providing the experimental IR spectra reported in the paper and to Solvay Specialty Polymers Italy SpA for providing the PTFE samples.

■ REFERENCES

- (a) Tommasini, M.; Castiglioni, C.; Milani, A.; Zerbi, G.; Radice, S.; Toniolo, P.; Grozzi, C.; Picozzi, R.; Di Meo, A.; Tonelli, C. *J. Fluorine Chem.* **2006**, *127*, 320–329. (b) Milani, A.; Tommasini, M.; Castiglioni, C.; Zerbi, G.; Radice, S.; Canil, G.; Toniolo, P.; Triulzi, F.; Colaianna, P. *Polymer* **2008**, *49*, 1812–1822. (c) Milani, A.; Castiglioni, C.; Di Dedda, E.; Radice, S.; Canil, G.; Di Meo, A.; Picozzi, R.; Tonelli, C. *Polymer* **2010**, *51*, 2597–2610.
- (a) Clark, E. S. *Polymer* **1999**, *40*, 4659–4665. (b) Clark, E. S. *J. Macromol. Sci., Part B: Phys.* **2006**, *45*, 201–213.
- Tadokoro, H. *Structure of Crystalline Polymers*; John Wiley and Sons: New York, 1979.
- Brown, R. G. *J. Chem. Phys.* **1964**, *40*, 2900–2908.
- (a) Rigby, H. A.; Bunn, C. W. *Nature* **1949**, *164*, 583–583. (b) Bunn, C. W.; Howells, E. R. *Nature* **1954**, *174*, 549–551.
- (a) Marx, P.; Dole, M. *J. Am. Chem. Soc.* **1955**, *77*, 4771–4774. (b) Villani, V. *Spectrochim. Acta* **1990**, *162*, 189–193.
- (a) Corradini, G.; Guerra, G. *Macromolecules* **1977**, *10*, 1410–1413. (b) Farmer, B. L.; Eby, R. K. *Polymer* **1981**, *22*, 1480–1486. (c) Kimmig, M.; Strobl, G.; Stuhn, B. *Macromolecules* **1994**, *27*, 2481–2495.
- Liang, C. Y.; Krimm, S. *J. Chem. Phys.* **1956**, *25*, 563–571.
- Moynihan, R. E. *J. Am. Chem. Soc.* **1959**, *81*, 1045–1050.
- (a) Koenig, J. L.; Boerio, F. *J. J. Chem. Phys.* **1969**, *50*, 2823–2829. (b) Hannon, M. J.; Koenig, J. L.; Boerio, F. *J. J. Chem. Phys.* **1969**, *50*, 2829–2836. (c) Koenig, J. L.; Boerio, F. *J. J. Chem. Phys.* **1970**, *52*, 4170–4171. (d) Boerio, F. J.; Koenig, J. L. *J. J. Chem. Phys.* **1970**, *52*, 4826–4829. (e) Boerio, F. J.; Koenig, J. L. *J. J. Chem. Phys.* **1971**, *54*, 3667–3677.
- Peacock, C. J.; Hendra, P. J.; Willis, H. A.; Cudby, M. E. A. *J. Chem. Soc. A* **1970**, 2943–2947.
- Piseri, L.; Powell, B. M.; Dolling, G. *Bull. Am. Phys. Soc.* **1971**, *16*, 311–?.
- (a) Zerbi, G.; Sacchi, M. *Macromolecules* **1973**, *6*, 692–699. (b) Masetti, G.; Cabassi, F.; Morelli, G.; Zerbi, G. *Macromolecules* **1973**, *6*, 700–707.
- Rae, P. J.; Dattelbaum, D. M. *Polymer* **2004**, *45*, 7615–7625.
- De Santis, P.; Giglio, E.; Liquori, A. M.; Ripamonti, A. *J. Polym. Sci., Part A* **1963**, *1*, 1383–1404.
- Farmer, B. L.; Eby, R. K. *Polymer* **1985**, *26*, 1944–1952.
- Quarti, C.; Milani, A.; Civalleri, B.; Orlando, R.; Castiglioni, C. *J. Phys. Chem. B* **2011**, *116*, 8299–8311.
- (a) Javier Torres, F.; Civalleri, B.; Meyer, A.; Musto, P.; Al bunia, A. R.; Rizzo, P.; Guerra, G. *J. Phys. Chem. B* **2009**, *113*, 5059–5071. (b) Javier Torres, F.; Civalleri, B.; Pisani, C.; Musto, P.; Al bunia, A. R.; Guerra, G. *J. Phys. Chem. B* **2007**, *111*, 6327–6335. (c) Al bunia, A. R.; Rizzo, P.; Guerra, G.; Javier Torres, F.; Civalleri, B.; Zicovich-Wilson, C. M. *Macromolecules* **2007**, *40*, 3895–3897. (d) Ferrari, A. M.; Civalleri, B.; Dovesi, R. *J. Comput. Chem.* **2010**, *31*, 1777–1784.
- (a) Zerbi, G.; Magni, R.; Gussoni, M.; Holland-Moritz, K.; Bigotto, A. B.; Dirlilikov, S. *J. Chem. Phys.* **1981**, *75*, 3175–3194. (b) Zerbi, G.; Minoni, G.; Tulloch, M. P. *J. Chem. Phys.* **1983**, *78*, 5853–5862. (c) Piazza, R.; Zerbi, G. *Polymer* **1982**, *23*, 1921–1928. (d) Zerbi, G. *Vibrational spectroscopy of very large molecules*. In *Advances in Infrared and Raman spectroscopy*; Clark, R. J. H., Hester, R. E., Eds.; Heyden: New York, 1984; Vol. 11, p 301. (e) *Modern Polymer Spectroscopy*; Zerbi, G., Ed.; Wiley-VCH: Weinheim, Germany, 1999.
- Dovesi, R.; Orlando, R.; Civalleri, B.; Roetti, C.; Saunders, V. R.; Zicovich-Wilson, C. M. Z. *Kristallogr.* **2005**, *220*, 571–273.

(21) Frisch, M. J.; Trucks, G. W.; Schlegel, H. B.; Scuseria, G. E.; Robb, M. A.; Cheeseman, J. R.; Scalmani, G.; Barone, V.; Mennucci, B.; Petersson, G. A.; et al. *Gaussian 09*, revision A.02; Gaussian, Inc.: Wallingford, CT, 2009.

(22) Becke, A. D. *J. Chem. Phys.* **1996**, *104*, 1040–1046.

(23) Schafer, A.; Huber, C.; Ahlrichs, R. *J. Chem. Phys.* **1994**, *100*, 5829–5835.

(24) Hehre, W. J.; Ditchfield, R.; Pople, J. A. *J. Chem. Phys.* **1972**, *56*, 2257–2261.

(25) (a) Grimme, S. *J. Comput. Chem.* **2004**, *25*, 1463–1473. (b) Grimme, S. *J. Comput. Chem.* **2006**, *27*, 1787–1795. (c) Civalleri, B.; Zicovich-Wilson, C. M.; Valenzano, L.; Ugliengo, P. *CrystEngComm* **2008**, *10*, 405–410.

(26) Since the different helical symmetries have been imposed in the calculations, we are not guaranteeing that the optimized chain structures correspond to true minima of the intramolecular potential energy surface. On the other hand, the full optimization of the geometry carried out on PTFE oligomers (see section 3.1.2) brings to the conclusion that the most stable conformation is characterized by torsional angles very close to the value of the 13_6 helix (163.4). In addition, an optimization with very small optimization steps and tight convergence criteria (“verytight” keyword used in the Gaussian input) from the starting geometry of the 15_7 helix (guess torsional angles fixed at $\theta = 165.6$) relaxes toward the most stable conformation (like the 13_6 helix).

(27) Smith, G. D.; Jaffe, R. L.; Yoon, D. Y. *Macromolecules* **1994**, *27*, 3166–3173.

(28) Rothlisberger, U.; Laasonen, K.; Klein, M. L.; Sprik, M. *J. Chem. Phys.* **1996**, *104*, 3692–3700.

(29) (a) D’Amore, M.; Auriemma, F.; De Rosa, C.; Barone, V. *Macromolecules* **2004**, *37*, 9473–9480. (b) D’Amore, M.; Talarico, G.; Barone, V. *J. Am. Chem. Soc.* **2006**, *128*, 1099–1108.

(30) As an alternative strategy for the investigation of the structure and energetic properties of the helix-reversal defect, it is possible to carry out calculations also on a 1D periodic model of the defect. This study would require a further wide computational study which goes beyond the aims of the present paper, and it is left for future investigations. On the other hand, the molecular model of the defect here adopted is long enough to give a reliable description of the relevant dynamical couplings responsible for the spectroscopic response.

(31) Milani, A.; Zanetti, J.; Castiglioni, C.; Di Dedda, E.; Radice, S.; Canil, G.; Tonelli, C. *Eur. Polym. J.* **2012**, *48*, 391–403.

(32) Sprik, M.; Rothlisberger, U.; Klein, M. L. *J. Phys. Chem. B* **1997**, *101*, 2745–2749.